Improving the fidelity of Mølmer–Sørensen entangling gates on long ion chains using temporal pulse shaping

Ali Binai-Motlagh

December 2020

Introduction

One way to generate entanglement between pairs of qubits in a trapped ion chain is through the Mølmer–Sørensen interaction. This scheme uses a pair of lasers, equally detuned above and below the qubit frequency ω_q by an amount $\pm\mu$. Considering a single ion and a single mode, the hamiltonian for this system is:

$$H = \frac{\omega_q}{2}\sigma_z + \omega_m a^\dagger a + \Omega\cos(k \cdot r - \omega_r t + \phi_r) + \cos(k \cdot r - \omega_b t + \phi_b) \tag{1}$$

Moving into a rotating frame with respect to the hamiltonian $H_0 = \frac{\omega_q}{2}\sigma_z + \omega_m a^\dagger a$ and working in the Lamb Dicke limit: $\eta = k\sqrt{\frac{\hbar}{2m\omega_m}} << 1$, one obtains:

$$H_{MS} = \frac{\Omega\eta}{2}\sigma_{\phi_s}\left[ae^{i(\mu-\omega_m)t+i\phi_m} + a^\dagger e^{i(\mu-\omega_m)t+i\phi_m}\right] \tag{2}$$

where $\phi_s \equiv (\phi_b + \phi_r + \pi)/2$ and $\phi_m \equiv (\phi_r - \phi_b)/2$ and $\sigma^+ = |1\rangle\langle 0|$ and $\sigma^- = |0\rangle\langle 1|$. To obtain this equation, it has further been assumed that $\frac{\Omega}{\mu} << 1$ so that several rapidly rotating terms, including those inducing off-resonant carrier transitions, can be neglected [1, 2]. Often, the red and blue detuned side-bands are induced through stimulated Raman transitions. In this case, the wave vector, k, is replaced by the difference in the wave vectors of the two Raman beams, Δk. This expression can be generalizaed to multiple ions and multiple motional modes by writing the ion positions in normal mode coordinates of the chain, and repeating a process similar to that for a single ion [1]:

$$H_{MS} = \sum_{\text{ion } i,\,\text{mode } m} \frac{\eta_{i,m}\cdot\Omega_i(t)}{2}\sigma_x^i \sin(\mu t)\left(a_m e^{-i\omega_m t} + a_m^\dagger e^{i\omega_m t}\right) \tag{3}$$

The Magnus expansion, $U(t) = e^{\Omega_1+\Omega_2+\cdots}$ can be used to derive the time evolution operator for this hamiltonian, where:

$$\Omega_1(t) = -i\int_0^t H(t')\mathrm{dt} \tag{4}$$

$$\Omega_2(t) = \frac{-1}{2}\int_0^t \mathrm{dt}'\int_0^{t'}[H(t'), H(t'')]\mathrm{dt}'' \tag{5}$$

Higher order terms in this expansion are not necessary as they involve nested commutators of this Hamiltonian at different times, which turn out to be zero in this case. Evaluating the integrals, one

obtains:

$$U(t) = \exp\Bigg[\sum_{i=1,m=1}^{N} (\alpha_{i,m}(t)\hat{a}_m^\dagger + \alpha_{i,m}(t)\hat{a}_m) \cdot \sigma_x^i + i \cdot \sum_{i=1,j=1}^{N} \chi_{i,j}(t)\sigma_x^i\sigma_x^j \Bigg] \tag{6}$$

where:

$$\alpha_{i,m}(t) \equiv -\eta_{i,m} \int_0^t \Omega_i(t^{'})\sin(\mu t^{'}) e^{i\omega_m t^{'}} \, \mathrm{dt}^{'} \tag{7}$$

$$\chi_{i,j}(t) \equiv -2 \sum_m \eta_{i,m}\eta_{j,m} \Bigg(\int_0^t \Bigg(\int_0^{t^{'}} \Omega_i(t^{'})\Omega_j(t^{''})\sin(\mu t^{'}) \, \sin(\mu t^{''}) \, \sin(\omega_m(t^{''} - t^{'})) \, \mathrm{dt}^{''} \Bigg) \mathrm{dt}^{'} \Bigg) \tag{8}$$

The first term in the exponent of $U(t)$ results in entanglement between motional mode m and ion i while the second term describes spin-spin entanglement between ions i and j.

If the ions were to start in the ground state of motion, the motional part of the above unitary, which is a displacement operator, maps the ground state to a coherent state $|\alpha_{i,m}(t)\rangle$ and causes the ions to follow closed trajectories in phase space as a function of time. This coherent state at the end of the gate depends on the mode m as well as the state of each qubit. As a result, the spin states of the ions can become entangled with its motion. This is undesirable because the goal of the above unitary is to entangle the spin of the two ions. The motional states can be thought of as ancillary qubits, necessary for the creation of the spin-spin entanglement, that are discarded or traced out at the end of the computation. If the motion is not in a product state with the spin, disposing of it will place the spins in a mixed state rather than the desired (pure) entangled state. Thus, to obtain the entangled state, one must tune the experimental parameters to return each motional mode simultaneously to the ground state (origin of phase space) at the end of the gate, i.e., to un-compute the ancilla.

Therefore, to turn the above interaction into a 2 qubit entangling gate, the following 2 conditions must be satisfied [2]:

1. $\alpha_{i,m}(\tau) = 0 \quad \forall \; i$ and modes m
2. $|\chi_{a,b}| = \frac{\pi}{4}$

Now assume that the rabbi frequency is non-zero for only the 2 ions involved in the interaction. That is, let $\Omega_a(t) = \Omega_b(t) = \Omega(t)$ for ions a and b and let $\Omega_i(t) = 0$ for all other ions i. In this case, the time evolution operator for the MS interaction simplifies to:

$$U(\tau) = e^{i\frac{\pi}{4}\sigma_x^a\sigma_x^b} = \begin{bmatrix} 1 & 0 & 0 & -i \\ 0 & 1 & -i & 0 \\ 0 & -i & 1 & 0 \\ -i & 0 & 0 & 1 \end{bmatrix} \tag{9}$$

applying this unitary to qubits initialized in $|00\rangle$ yields a Bell state: $U(\tau)|00\rangle = \frac{1}{\sqrt{2}}(|00\rangle - i|11\rangle)$.
Assuming that that the interaction only couples to the N modes with frequencies closest to the detuning μ, the first requirement represents a set of $2N$ constraints, N for the real part of $\alpha_{i,m}(\tau)$ and N for the imaginary part. This is a fair assumption as long as the Rabbi frequency is small enough so that it does not appreciably modify the other $2N$ modes further from the laser detuning. It should be noted that if condition 1 is satisfied for ion a, then it is also satisfied for ion b as the only change between the equations for the two ions is the Lamb-Dicke factor. Therefore, the two above conditions represent a set of 2N + 1 constraints that must be satisfied by tuning the experimental parameters. For 2 ions interacting with lasers of constant amplitude, the phase space trajectories can be closed at the end of the pulse through a proper choice of the detuning μ. To see this first evaluate equation 7 for a constant Ω, this yields:

$$\alpha_{i,m} = \frac{\eta_{i,m}}{\mu^2 - \omega_m^2}\left[e^{i\omega_m t}(\mu\cos(\mu t) - i\omega_m\sin(\mu t)) - \mu\right]$$

When $\delta_m \equiv \mu - \omega_m << \mu + \omega_m$ the trajectories become circular:

$$\alpha_{i,m} = \frac{\eta_{i,m}\Omega_i}{2\delta_m}\left(e^{i\delta t} - 1\right)$$

From this we can see that if we were to, for example, pick μ so that it is exactly half way between the two motional modes then $\delta_1 = \delta_2$ and both trajectories close by choosing the gate time to be an integer multiple of $\frac{2\pi}{\delta_1}$. This is visualized in figure 1.
The second condition can be satisfied by tuning the constant rabbi frequency Ω. For larger chains, involving many motional modes, an artful choice of the detuning is not sufficient to close all phase space trajectories. Even for the case of 2 ions, having the trajectories close only at a discrete set of detunings is undesirable as small fluctuations in the detuning can prevent the trajectories from reaching the origin at the end of the gate. These problems can be addressed by introducing additional experimental control parameters. For example, the amplitude, frequency or phase of the laser beams can be made functions of

time. Here I explore how amplitude modulation can be used to satisfy the 2 conditions outlined above, yielding near unity fidelity at all detunings. This work is primarily based on Chapter 4 of T.A. Manning's thesis [2].

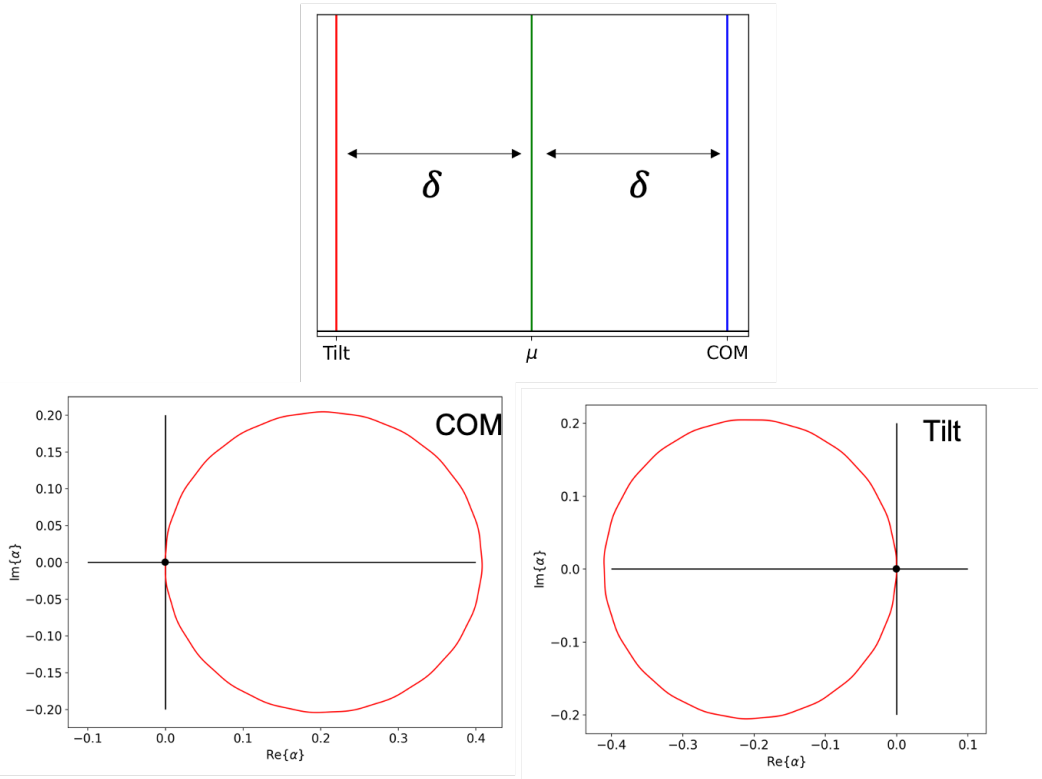

Figure 1: Phase space trajectories for the Centre of mass (COM) and Tilt modes when the detuning μ is placed exactly in the middle of the two mode frequencies. By picking the gate time to be an integer multiple of $\frac{2\pi}{\delta}$ both trajectories can be simultaneously closed.

Amplitude modulation theory

In this technique, a pulse of duration τ is divided into S equal segments:

$$\Omega(t) = \begin{cases} \Omega_1 & 0 \leq t \leq \frac{\tau}{S} \\ \Omega_2 & \frac{\tau}{S} \leq t \leq \frac{2\tau}{S} \\ \Omega_3 & \frac{2\tau}{S} \leq t \leq \frac{3\tau}{S} \\ \dots & \\ \Omega_S & \frac{(S-1)\tau}{S} \leq t \leq \tau \end{cases} \tag{10}$$

In this case, the phase space closure condition becomes:

$$\sum_{s=1}^{S} \Omega_s C_{m,s}^{l} = 0 \quad \text{where} \quad C_{m,s}^{l} = -\eta_{l,m} \int_{\frac{s-1}{S}\tau}^{\frac{s}{S}\tau} \sin(\mu t) e^{i\omega_m t} \mathrm{dt} \tag{11}$$

where $l \in a, b$ indexes the ions. For the segmented pulse, the geometric phase criterion becomes:

$$\sum_{s=1}^{S} \sum_{s'=1}^{s} \Omega_s \Omega_{s'} D_{s,s'} = \frac{\pi}{4} \tag{12}$$

where $D_{s,s'}$ is defined as:

$$\sum_{m=1}^{N} \eta_{a,m} \eta_{b,m} \int_{\frac{s-1}{S}\tau}^{\frac{s}{S}\tau} \mathrm{dt}_1 \int_{\frac{s'-1}{S}\tau}^{\frac{s'}{S}\tau} \sin(\mu t 1) \sin(\mu t_2) \sin(\omega_m (t_2 - t_1)) \, \mathrm{dt}_2. \tag{13}$$

when $s^{'} < s$. When $s^{'} = s$ we have:

$$\sum_{m=1}^{N} \eta_{a,m} \eta_{b,m} \int_{\frac{s-1}{S}\tau}^{\frac{s}{S}\tau} \mathrm{dt}_1 \int_{\frac{s'-1}{S}\tau}^{t_1} \sin(\mu t_1) \sin(\mu t_2) \sin(\omega_m (t_2 - t_1)) \, \mathrm{dt}_2. \tag{14}$$

The integral in equation 11 can be evaluated analytically, yielding:

$$-\eta_{l,m} \int_{t_0}^{t_1} \sin(\mu t) e^{i\omega_m t} \mathrm{dt} = \frac{\eta_{i,m}}{\mu^2 - \omega_m^2} \left[e^{i\omega_m t_1} (\mu \cos(\mu t_1) - i\omega_m \sin(\mu t_1)) - e^{i\omega_m t_0} (\mu \cos(\mu t_0) - i\omega_m \sin(\mu t_0)) \right] \tag{15}$$

This is also true for equations 13 and 14. However, in order to avoid making mistakes, a computer algebra software was used to evaluate them and translate them to python code. Equations 11 and 12 can be written in matrix form as:

$$\mathbf{C_l \Omega} = \mathbf{0} \tag{16}$$

$$\mathbf{\Omega^T D \Omega} = \frac{\pi}{4} \tag{17}$$

Where $\mathbf{C_l}, l \in \{a, b\}$ is the matrix whose (m, s) element is $C_{m,s}^{l}$, $\mathbf{\Omega}$ is an S dimensional column vector whose elements are the pulse amplitudes and D is a matrix whose $(s, s^{'})$ element is $D_{s,s'}$. To obtain a solution for Ω, one would solve the linear system: $\mathrm{Re}\{\mathbf{C_l \Omega}\} = \mathbf{0}$ $\mathrm{Im}\{\mathbf{C_l \Omega}\} = \mathbf{0}$. This system is a homogeneous

system of $2N$ equations and is guaranteed to have a non-trivial solution when there are at least $2N + 1$ pulse segments. A solution $\mathbf{\Omega}$ for the matrix $\mathbf{C_a}$ will also be in the null space of $\mathbf{C_b}$. Given a non-trivial solution $\mathbf{\Omega}$ and a scalar c, $c\mathbf{\Omega}$ is also a solution. So to also satisfy the geometric phase condition 12 we can simply normalize $\mathbf{\Omega}$ so that $\mathbf{\Omega^T D \Omega} = \frac{\pi}{4}$.

It turns out that one can get away with using fewer than $2N + 1$ pulse segments and still attain a fidelity near unity. This is because the real and imaginary parts of the linear system are not independent and so some of the equations are redundant [3]. As a result N + 1 segments may be sufficient for obtaining an exact solution, i.e. a solution that closes all phase space trajectories. However, when there are fewer than $2N + 1$ segments the linear system has no non-trivial solution. In this case a good $\mathbf{\Omega}$ can be found through numerical optimization by using the infidelity, $1 - F$ as the cost function and $\mathbf{\Omega}$ as its parameters. In this case, we may not be able to close all phase space trajectories but the optimization finds Rabbi frequencies that close the "more influential" ones. Note that this is only the case if the gate times are long enough so that the rabbi frequencies can be made sufficiently small to only significantly excite the N modes closest to μ. For shorter gate times, more segments may be necessary [4].

We would like to generate the sate $|\psi_{\text{ideal}}\rangle = \frac{1}{\sqrt{2}}(|00\rangle - i\,|11\rangle)$ using the interaction described by 2 which yields the state $\rho(\tau) = Tr_{\text{motion}}\left[U(\tau)^\dagger \rho(0) U(\tau)\right]$. The distance between the two states can be measured by the fidelity, $F = Tr\left(\rho(\tau)\,|\psi_{\text{ideal}}\rangle\,\langle\psi_{\text{ideal}}|\right)$. A fidelity of 1 implies that the desired pure state $|\psi_{\text{ideal}}\rangle$ and the state generated by the MS interaction, $\rho(\tau)$, are identical. Taking the initial internal state of the ions to be: $\rho_{ion}(0) = |00\rangle_z$ and assuming that each mode is in a thermal distribution with average phonon number $\bar{n}_m$:

$$\rho_m(0) = \sum_{n=0} \left(\frac{n}{1-\bar{n}_m}\right)^n e^{\frac{-\hbar\omega_m}{k_B T}}\,|n\rangle\,\langle n| \tag{18}$$

where k_B is the Boltzmann constant, T is the temperature and $k_B T \equiv \hbar\omega_m \bar{n}_m$. We can then write $\rho(0) = \rho_{\text{ion}}(0) \otimes \left(\bigotimes_m \rho_m(0)\right)$. Starting with this state one can then show that the fidelity is:

$$F = \frac{1}{8}(2 + 2\,\sin(2 \cdot \chi_{a,b})(\Gamma_a + \Gamma_b) + \Gamma_+ + \Gamma_-) \tag{19}$$

where $\Gamma_l = e^{-\sum_{m=1}^{N} |\alpha_{l,m}(\tau)|^2 \cdot \beta_m/2}$ and $\Gamma_\pm = e^{-\sum_{m=1}^{N} |\alpha_{a,m}(\tau) \pm \alpha_{b,m}|^2 \cdot \beta_m/2}$ where $\beta_m = \coth\left(\ln(1 + \frac{1}{\bar{n}_m})\right)$.

We can then use constrained numerical optimization techniques to minimize the cost function $f(\mathbf{\Omega}) = 1 - F(\mathbf{\Omega})$ and determine the amplitudes required for each segment that yield the highest fidelity. To clarify

what the optimization does to the phase space trajectories, consider the approximate fidelity in the limit where $1 - F << 1$ and when $\chi_{a,b} = \frac{\pi}{4}$:

$$F \approx 1 - \frac{1}{4} \sum_{m=1}^{N} |\alpha_{a,m}(\tau)|^2 + |\alpha_{b,m}(\tau)|^2 \tag{20}$$

From this we see that optimization favours phase space trajectories, for all ions and modes, that are close to the origin at the end of the gate. The numerical optimization technique used here differs slightly from the techniques used in [2, 4]. Here the full un-approximated infidelity is used as the cost function while [2, 4] use an approximation valid for small $1 - F$. Reference [4] also includes a term in the fidelity that accounts for off-resonant carrier transitions. The two techniques outlined above (solving the linear system and numerical optimization) will be applied to chains of 2 and 5 ions in the following sections.

Results for a 2 ion chain

The simulations are performed on a chain of $^{171}Yb^{+}$ ions. It is assumed that Raman transitions are implemented using a pair of counterpropagating laser beams with $\lambda = 355$ nm. The transverse trap frequency is taken to be $\omega_x = \omega_y = 4.38$ MHz and the axial frequency is taken to be $\omega_z = 600$ kHz as in reference [2]. The gate time is set to $\tau = 104$ μs. A simplifying assumption implicit in the above analysis was that the MS interaction only excites the N modes that are closest in frequency to the chosen detuning. In this case the transverse modes will be used to implement the entangling gate.

The main results for the 2 ion chain are shown in figure 2. Figure 2 (a) plots the optimal fidelity as a function of detuning for a constant pulse for average phonon numbers, $\bar{n} = 0, 2, 10$. As expected, the highest fidelities are attained for $\bar{n} = 0$. The bandwidth over which the fidelity is large is also broadest for this case. The points at which the fidelities are near 1 correspond to detunings at which the phase space trajectories for both modes can be simultaneously closed. This is consistent with the results of [2]. Unlike the results of [2] where the peak fidelity is near 1 for all values of the average phonon number, we see that the peak fidelity decreases with $\bar{n}$. The exact reason for this inconsistency could not be identified. However, the equation for the D matrix on page 101of [2] is incorrect. This may have been the source of the inconsistency. Figure 2 (b) plots the optimal fidelity as a function of detuning for a 5 segment pulse. In this case we have enough control parameters to close all phase space trajectories and as a result a fidelity of 1 can be achieved at all detunings. Figure 2 also shows the optimal Rabbi frequencies for

the constant and 5 segment pulses. For the 5 segment pulse the absolute value of the largest amplitude is plotted at each detuning. Comparing the two we see that the Rabbi frequencies are on the same order of magnitude for most detunings. This is desirable because it means that the maximum required Rabbi frequency is small enough to make the modulation technique viable.

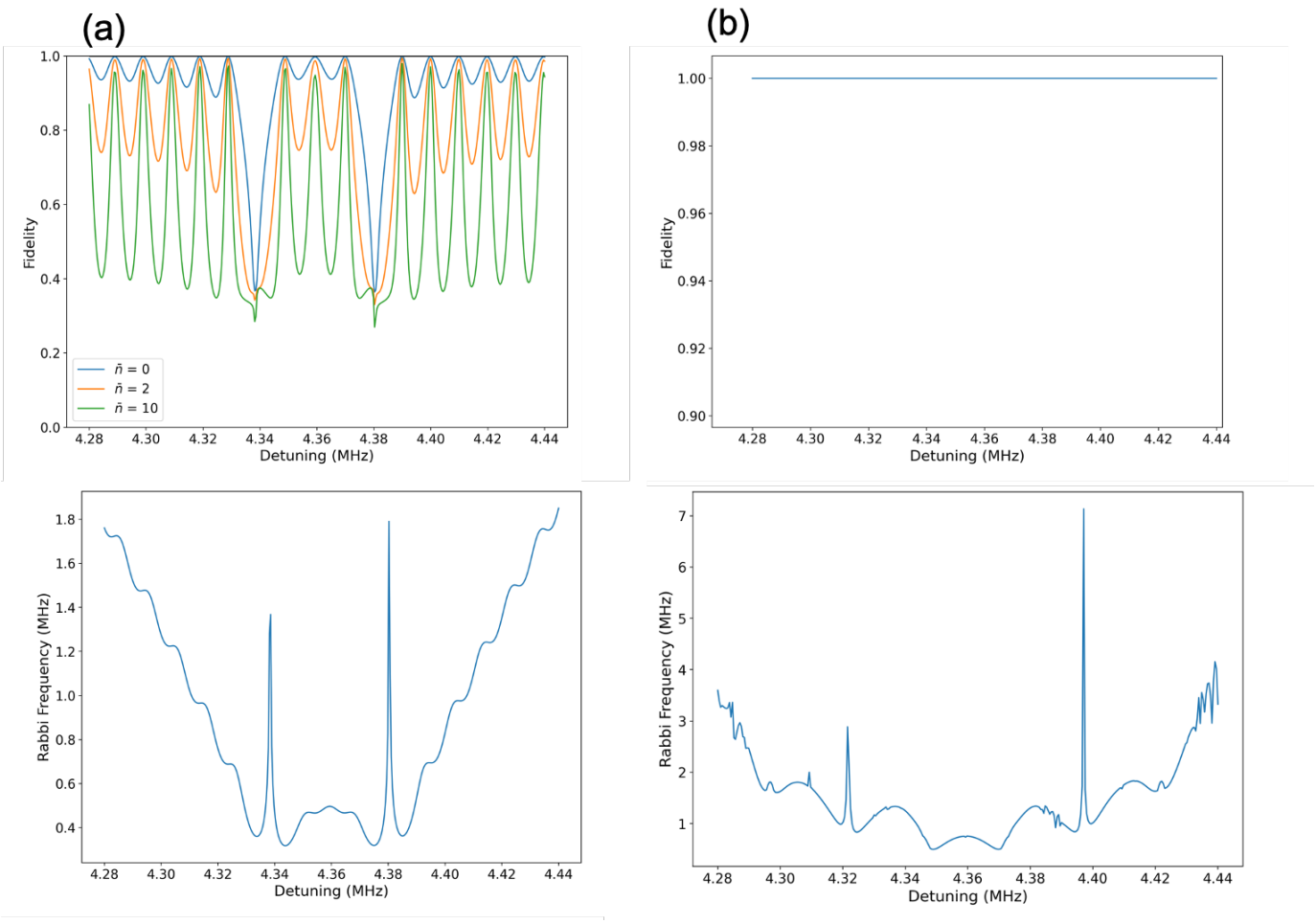

Figure 2: Optimal Fidelity and Rabbi frequency as a function of detuning μ for a constant pulse (a). Optimal fidelity and magnitude of the maximum Rabbi frequency of a 5 segment pulse as a function of detuning (b). With the extra control parameters afforded by the 5 segment pulse, the fidelity can be made very close to 1, without a substantial increase in the maximum required Rabbi frequency.

The phase space trajectories for the 5 segment pulse and a detuning $\mu = 4.362$ MHz are shown in figure 3. Figure 3 (a) and (b) plot the phase space trajectories for the center of mass and tilt modes of ion 1 respectively. The trajectories for the second ion look very similar, all ending at the origin at the end of the pulse. Figure 3 (c) is a plot of the optimal 5 segment pulse at $\mu = 4.362$ MHz. The pulse is symmetric at its center point, suggesting that 2N + 1 unique segments are not necessarily needed to meet the phase

space closure criterion. This is expected because, as discussed above, the real and imaginary parts of the C matrix are not independent.

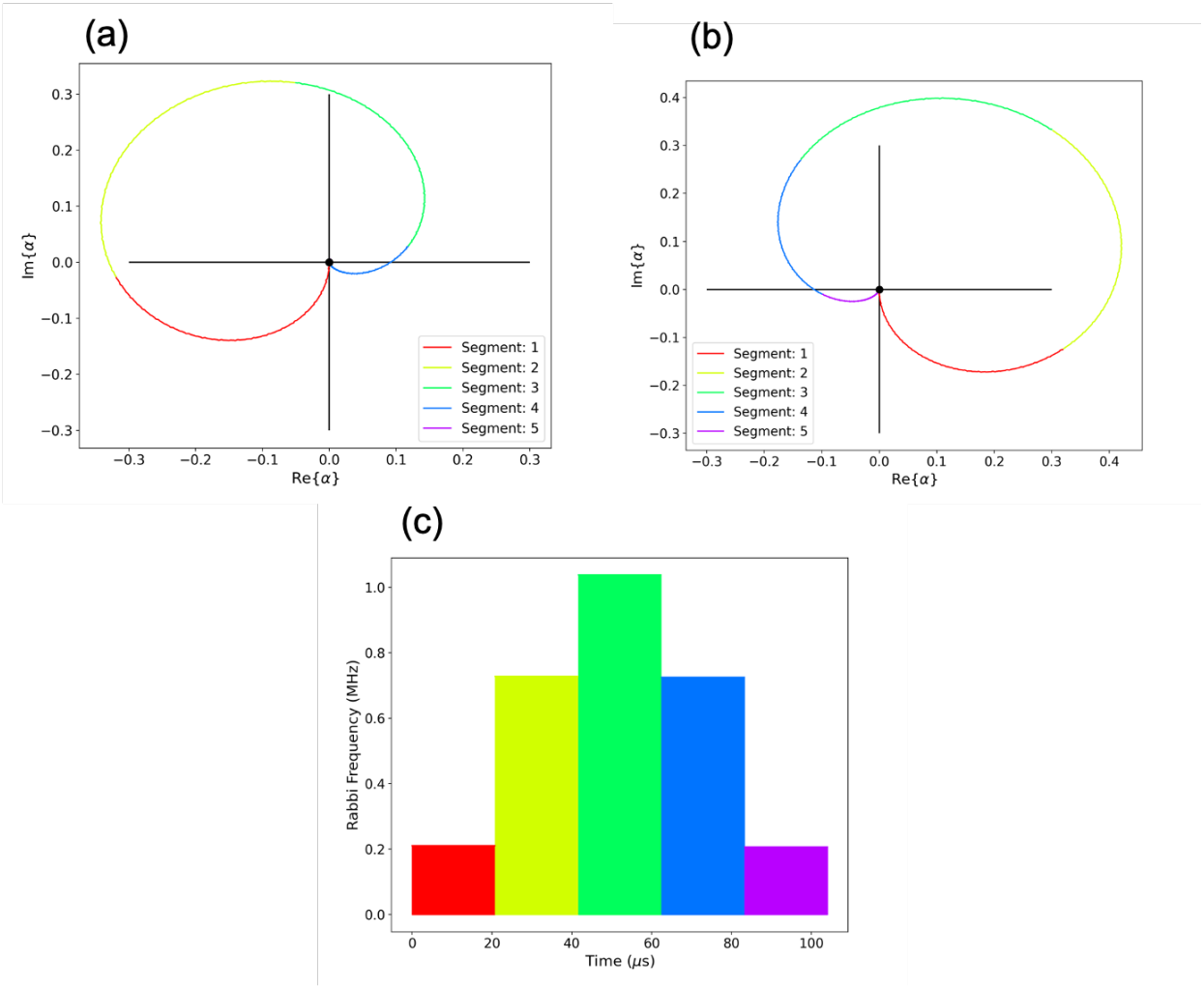

Figure 3: Phase space trajectories for the center of mass mode (a) and Tilt mode (b) for a two ion chain at a detuning of $\mu = 4.362$ MHz. As desired, both trajectories close at the end of the gate. This is indicated by the black dot at the origin. (c) shows the optimal pulse shape as a function of time.

Results for a 5 ion chain

In this section we will repeat the same analysis for a 5 ion chain. In this case $2N + 1 = 11$ and so at most 11 pulse segments are required to close all phase space trajectories. We will also explore the performance of 5 and 9 segment pulses obtained through numerical optimization. Again following the experimental parameters provided in [2] we will set $\omega_x = \omega_y = 2.59$ MHz and $\omega_z = 315$ kHz. we will set the gate time to $\tau = 200$ μs.

Figure 4 plots the fidelity and Rabbi frequency as a function of detuning for a constant pulse (blue) and

an 11 segment pulse. Similar to what was observed in the two ion case, the fidelity for a constant pulse reaches values near unity at a set of discrete detunings and dips to very low values when μ is near one of the mode frequencies ω_m. With an 11 segment pulse, a fidelity of unity is obtained at all detunings. This is attained, as with the 2 ion case, without a substantial increase in the maximum Rabbi frequency at most detunings.

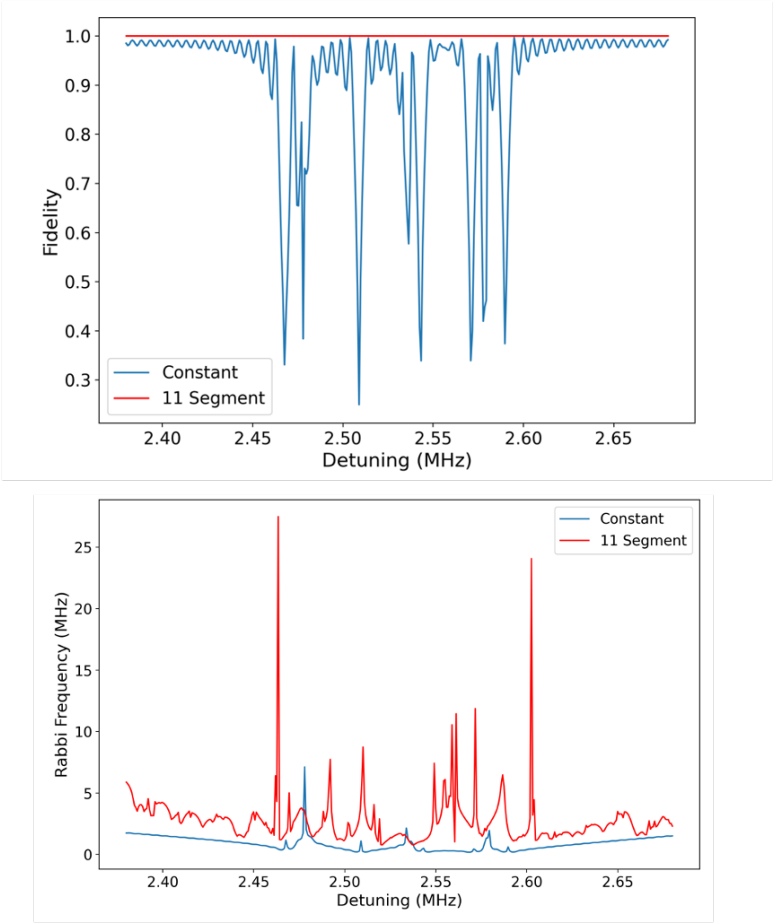

Figure 4: Optimal fidelity and Rabbi frequency as a function of detuning for a constant (blue) and an 11 segment pulse (red), in a 5 ion chain. For the 11 segment pulse we have plotted the absolute value of the maximum Rabbi frequency at each detuning.

Figure 5 shows the optimal pulse and resulting phase space trajectories for one of the optimal 11 segment pulses at a detuning of $\mu = 2.49$ MHz. We see that the phase space trajectories for the motional modes with frequency $\omega_m = 2.54$ MHz and 2.51 MHz close at the end of the pulse. This is also true for all other modes. The optimal pulse shape is symmetric about the center point at 100μs, suggesting again that we can obtain a fidelity close to unity with fewer than 11 pulse segments. Strictly speaking, the symmetry on its own is not enough to assert that we can get away with fewer pulse segments. What it implies, if we believe it to be a general trend, is that for an S segment pulse, we can get away with

only optimizing with respect to S/2 parameters. This makes the optimization problem simpler, but still, S segments are needed to satisfy the phase space closure constraints. Nevertheless, as we shall see, it turns out that less than 2N+1 pulse segments will suffice. [1]

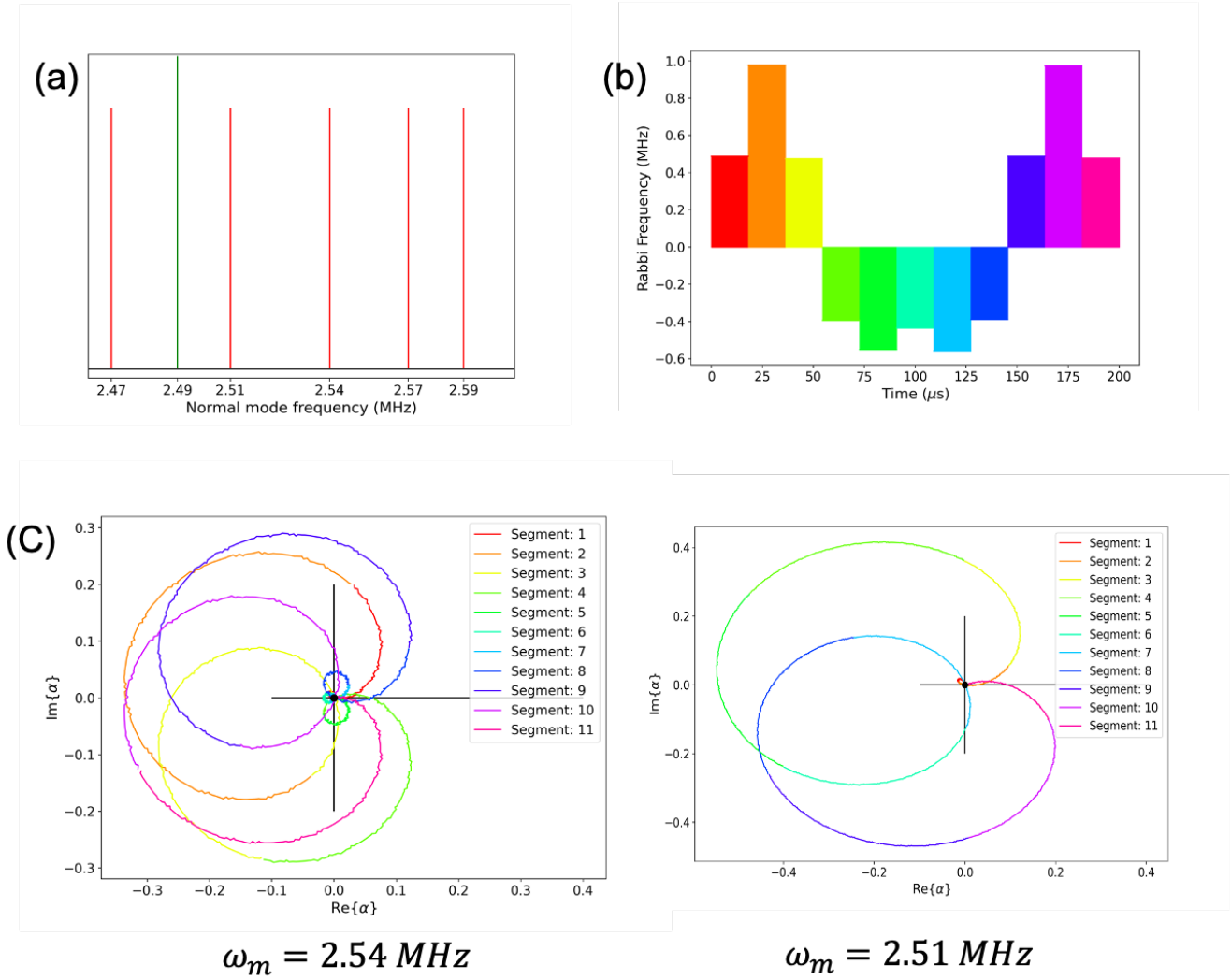

Figure 5: Sample phase space trajectories for the 11 segment pulse for a detuning μ = 2.49 MHz. (a) shows the position of the laser detuning (green) relative to the 5 transverse motional mode frequencies (red). The optimal pulse shape is shown in (b). (c) shows the phase space trajectories for 2 of the modes.

To test this idea, the fidelity (equation 19) was minimized with respect to the amplitudes of 5 and 9 segment pulses. The optimization algorithm Differential Evolution was used to carry out the minimization. Several other algorithms, including Nelder-Mead and Sequential Least Squares Programming (SLSQP) were tested. However it was found that Differential Evolution yielded the highest fidelities in the shortest amount of time. The results for 9 and 5 segment pulses are shown in figure 6. This plots the fidelities and

[1]This last bit was added in response to my bad answer to Elijah's question.

the absolute value of the maximum Rabbi frequencies as a function of detuning. For the 5 segment pulse, we see that the fidelity is nearly 1 at nearly all detunings except at a set of values near the motional mode frequencies. These dips may have been caused by stopping the optimization prematurely and may clear out if the optimizer was executed several more times with random initial conditions. For the 9 segment pulse, a fidelity near unity was obtained at all detunings. Overlooking the slight dips in the 5 segment pulse, similar fidelities were attained with both pulses. This indicates that the 2N+1 segment full control pulse is unnecessary and we can implement a robust entangling gate, even with as little as 5 segments. Figure 6 also plots the rabbi frequencies of both pulses as a function of detuning. For the 5 segment pulse, the absolute value of the maximum Rabbi frequency is on the order of that required for a constant pulse and has a profile that resembles all other Rabbi frequency plots. The 9 segment Rabbi frequency is more erratic and unstructured. This same qualitative behaviour is present in the data of reference [2], but in our case the spikes in rabbi frequency are larger.

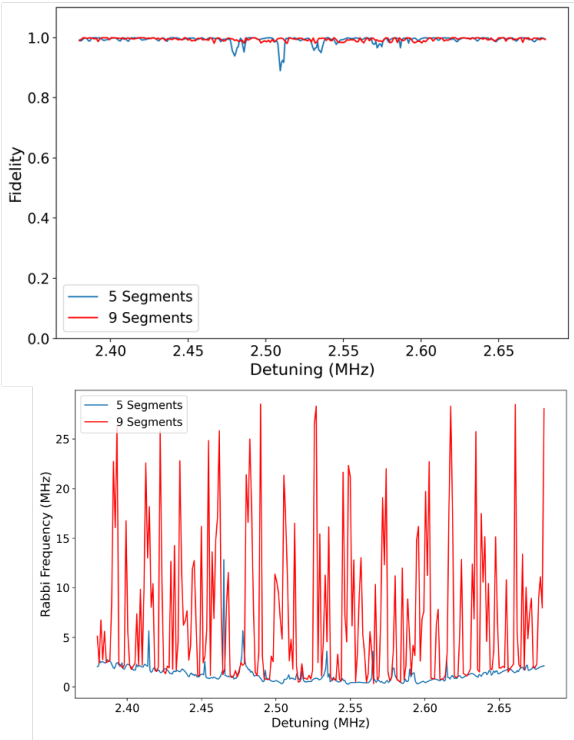

Figure 6: Optimal fidelity and absolute value of the maximum Rabbi frequency as a function of detuning for a 5 segment (blue) and a 9 segment pulse (red), for a 5 ion chain.

Figure 7 plots sample phase space trajectories and pulse shapes for both the 5 and 9 segment pulses at a detuning $\mu = 2.49$ MHz. The sample trajectories plotted are for the motional mode with frequency $\omega_m = 2.51$ MHz. Both trajectories close at the end of the gate as required to maximize the fidelity. These

results are qualitatively similar to those presented in references [4, 5]. It should be noted that the results presented herein are for entanglement between a pair of ions at the end of the chain and the phase space trajectories plotted are only for one ion in the pair. However, similar results were obtained for all other pairs of ions tested. The symmetry present in the 11 segment pulse is also present in the 5 and 9 segment pulses. This is not a general rule; other optimal pulse solutions were obtained that were not symmetric about the centre of the pulse.

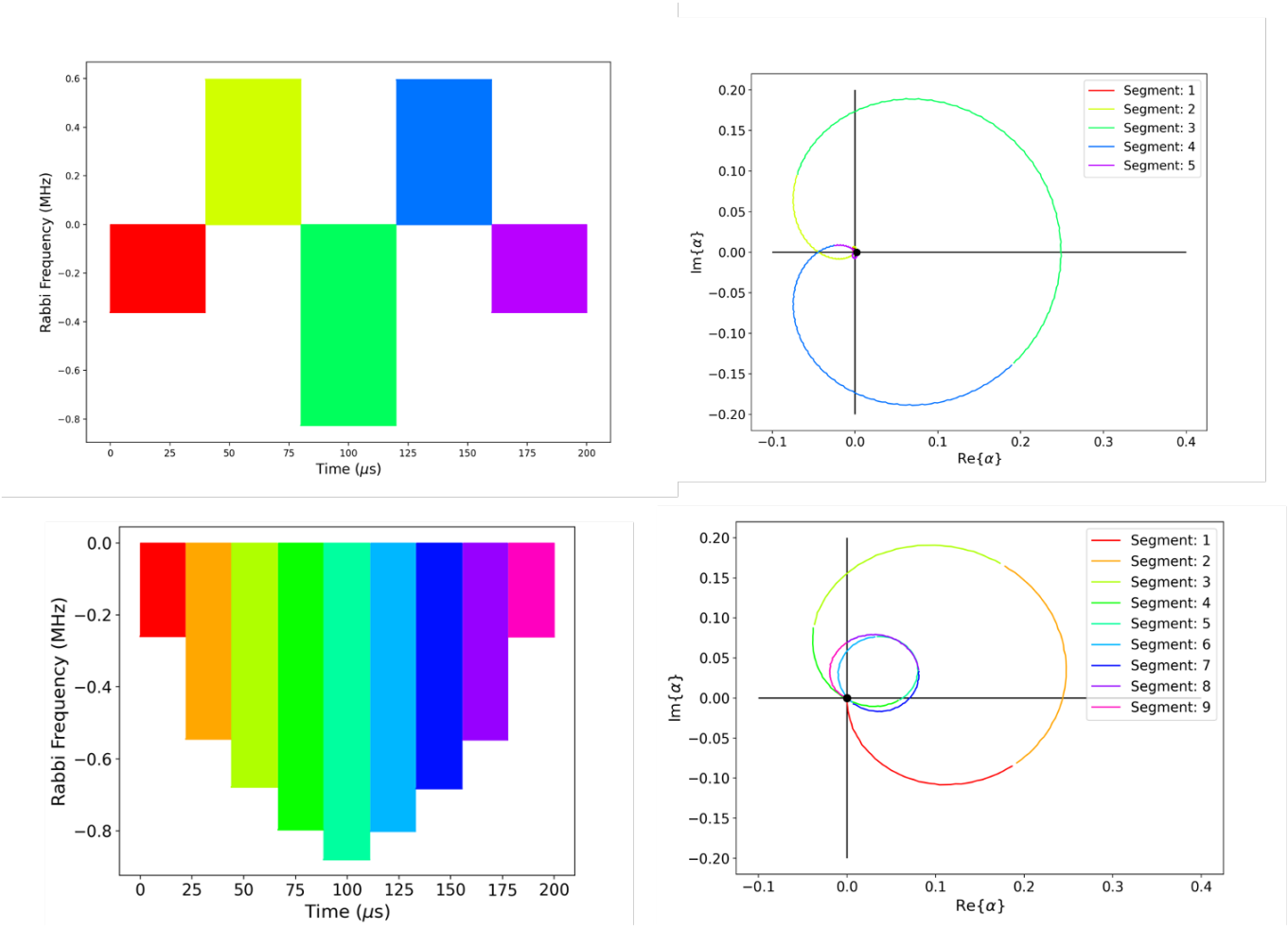

Figure 7: Sample plots of the optimal pulse shape and phase space trajectories for a 5 and 9 segment pulse at $\mu = 2.49$ MHz. The phase space trajectories for the $\omega_m = 2.51$ MHz mode are shown.

Another advantage afforded by using a multi-segment pulse is that it can be robust to variations in detuning [5], due to noise in the laser frequency, given a judicious choice for its value. Figure 8 (a) plots the optimal Rabbi frequencies of each segment of the 9 segment pulse as a function of detuning. To make the gate resistant to variations, a detuning where the optimal Rabbi frequency is relatively constant for all pulse segments should be chosen. In this case, 2.5385 MHz was chosen, denoted by the dashed

vertical line. Figure 8 (b) plots the fidelity of the 9 segment pulse, using the optimal rabbi frequencies obtained at this particular detuning. For detunings away from 2.5385 MHz the chosen rabbi frequencies are no longer optimal. However, because the optimal solution remains relatively constant over a range of approximately 2 kHz, the fidelity of the 9 segment pulse remains large, compared to that of the constant pulse which sharply drops beyond the $\mu = 2.5385$ MHz optimal point.

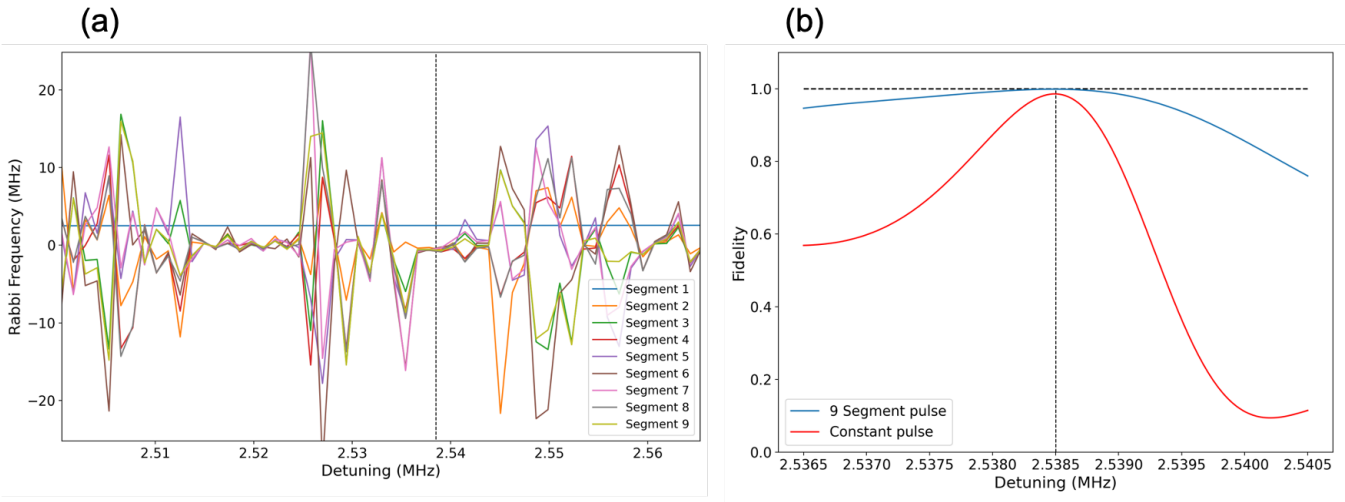

Figure 8: (a) Optimal Rabbi frequencies of all portions of the 9 segment pulse. The dashed vertical line denotes a point, around which the optimal Rabbi frequency is relatively constant over a range of a few kHz. (b) Plot of the fidelity as a function of detuning over a 4 kHz range using the optimal Rabbi frequency at $\mu = 2.5385$ MHz.

Conclusion

The presented results demonstrate the necessity of extra degrees of freedom for a high fidelity implementation of XX-entangling gates based on the MS interaction. In this case the extra control parameters were obtained by modulating the amplitude of the lasers as a function of time. We have shown that unity fidelity can be attained using multi-segment pulses in chains of 2 and 5 ions. In the future, techniques utilizing time-dependent frequencies or phases [6, 7] may be used in conjunction with amplitude modulation to potentially make the gate more robust. It is important to note that all of the reported fidelities represent an upper-bound on the true experimental fidelities. The calculated fidelities describe the distance between the desired bell state and the state obtained given the approximate interaction Hamiltonian H_{MS} and perfect experimental parameters. This does not take into account potential noise in the frequency, amplitude or phase of the Raman lasers. Our model Hamiltonian H_{MS} is also an idealization, neglecting interactions such as off-resonant carrier transitions [4].

References

[1]C. R. Senko, "Dynamics and excited states of quantum many-body spin chains with trapped ions", PhD thesis (University of Maryland College Park, 2014).

[2]T. A. Manning, "Quantum information processing with trapped ion chains", PhD thesis (University of Maryland College Park, 2014).

[3]S. Debnath, "A programmable five qubit quantum computer using trapped atomic ions", PhD thesis (University of Maryland College Park, 2016).

[4]S. Miller, *Optical pulse shaping for trapped-ion quantum computing with integrated photonics*, 2019.

[5]T. Choi, S. Debnath, T. A. Manning, C. Figgatt, Z.-X. Gong, L.-M. Duan, and C. Monroe, "Optimal quantum control of multimode couplings between trapped ion qubits for scalable entanglement", Physical Review Letters **112** (2014).

[6]T. J. Green and M. J. Biercuk, "Phase-modulated decoupling and error suppression in qubit-oscillator systems", Phys. Rev. Lett. **114**, 120502 (2015).

[7]P. H. Leung, K. A. Landsman, C. Figgatt, N. M. Linke, C. Monroe, and K. R. Brown, "Robust 2-qubit gates in a linear ion crystal using a frequency-modulated driving force", Phys. Rev. Lett. **120**, 020501 (2018).